Int. J. Electrochem. Sci., 10 **(2015)** 8484 - 8496

International Journal of
ELECTROCHEMICAL
SCIENCE
www.electrochemsci.org

Electrochemical-Fractal Model Versus Randles Model: A Discussion About Diffusion Process

Gabriel A. Ruiz[1,*] *and Carmelo J.Felice*[1,2]

[1] Laboratorio de Medios e Interfases (LAMEIN), Universidad Nacional de Tucumán, Tucumán, Argentina.
[2] Consejo Nacional de Investigaciones Científicas y Técnicas (CONICET), Argentina.
[*]E-mail: gruiz@herrera.unt.edu.ar

Received: 8 June 2015 / *Accepted:* 31 JUly 2015 / *Published:* 26 August 2015

This paper presents an integral electrical model (IEM) of an electrode-electrolyte interface (EEI), which integrates geometrical and electrochemical aspects. It includes the diffusion of ionic species onto the electrode, the charge transference, the charge double layer, and the roughness degree of the electrode. The EEI impedance is electrically modelled by using a parallel connection between a double layer capacitance C_{dl} and a charge transference resistance R_{ct}. The diffusion impedance is also modelled through an electrical circuit which consists of a resistance R_D and a capacitance C_D, both connected in parallel. R_D models the energy dissipation and C_D models the space distribution of the electrical charge. The parallel takes into account the fact that both phenomena occur at the same place and simultaneously. This model can be used by professors and teachers to explain and distinguish important concepts in the field of electrochemistry as the difference between the ions movement into the EEI (charge transfer) and ions movement into the diffusion layer. This difference is not clear, for example, in the Randles circuit, where diffusion impedance (Warburg element) and C_{dl} were connected in parallel. This implies that diffusion and the diffuse layer take place in the same space and simultaneously. The Ion movement from the medium to the external Helmholtz layer is a process previous to the charge transfer reaction and the double layer charging process. That is the reason why the EEI and diffusion impedances have been connected in series. Most importantly, both Randles and IEM models, qualitatively exhibit the same behaviour with frequency and in the complex plane.

Keywords: Electrode-Electrolyte Interface – Diffusion – Roughness Electrode.

1. INTRODUCTION

In 1899 Warburg was the first researcher who interpreted the ionic species diffusion from and to an electrode-electrolyte interface (EEI) as a charge transport process and he represented this process as electrical impedance [1]. Based on the fact that the polarization voltage is delayed with respect to

the current which circulated between the electrodes, he considered that the impedance should have a capacitive character, and therefore he proposed a series RC model.

Randles [2] was able to synthesize an equivalent circuit consisting of an electrolytic resistance R in series with the parallel connection between the double-layer capacitance C_{dl} and the series combination R_{ct}-Z_W (Fig. 1). R_{ct} is the charge transfer resistance and Z_W is called Warburg element and is calculated as $A_W/(i\omega)^{0.5}$, where A_W is the Warburg coefficient, i is the imaginary unit, and $\omega = 2\pi f$ is the angular frequency. This equivalent circuit models electrochemical reactions of an EEI in presence of semi-infinite linear diffusion of electroactive species to metallic electrodes.

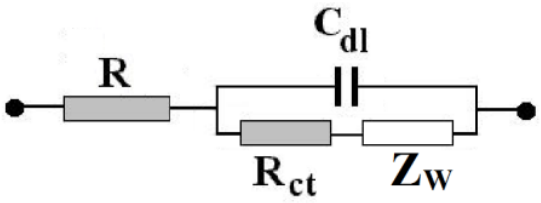

Figure 1. Randles circuit.

Randles' model, Warburg's and others authors ones [3]–[4], assumed that the electrode is totally flat, and therefore, they do not incorporated the roughness of the electrode. Taylor and Gileadi [5] proposed a variation of Warburg's model which presents some deficiencies by assume that Nernst diffusion layer under step voltage conditions is the same for sinusoidal disturbances.

Mc Adams and Jossinet [6] have represented the EEI impedance with an equivalent circuit which consists of a CPA element (Z_{CPA}) in parallel with a resistance (R_{tc}). They attribute Z_{CPA} to the double layer capacitance and its effects of superficial adsorption.

Liu' model [7] takes into account the surface geometry of the electrode. His model proposes an electrical circuit derived on the structure of a fractal network by using Cantor's bars. Its limitation is that it incorporates C_{dl} as the only electrochemical parameter, without taking into account the charge transference and the diffusion processes. When the roughness increases, the interface impedance also increases, contrary to what is experimentally observed.

Nyikos and Pajkossy [8]–[13] modelled the roughness of a metal electrode by using the self-similar fractal structure, the profile of which is Von Koch's curve shaped instead of Cantor's bars' as Liu has done it.

There are other electrode-electrolyte interface models in the literature which integrate electrochemical and geometrical parameters, such as Ruiz-Felice [14]–[15], however this model does not include transport phenomena, such as diffusion.

De Levie [16] generalized the Nyikos y Pajkossy's model by rewriting the interface admittance which includes faradic processes, mass transport, and coupled chemical reactions.

Recently, other authors [17]–[19] have also electrically modelled their systems by using an equivalent circuit consisting of a Z_{CPA} in parallel with a series combination of R_{ct}-Z_W.

This paper presents an integral electrical model (IEM) of an EEI which, differently from other

previous models (Warburg; Taylor and Gileadi; Randles; Liu; De Levie; McAdams; Finšgar; Mahjani), takes into consideration the spatial location and the time distribution of the electrochemical phenomena of an EEI. It also includes the fractal geometry and uses senoidal overpotentials of an applied signal. The model describes the interface performance in linear and non linear zones, and it does not use fractional exponents or fractal dimensions, therefore, it permits a better physical interpretation of all the underlying electrochemical phenomena. IEM takes into account that physically speaking, the ion distribution from the medium to the external Helmholtz layer is a process previous to the charge transfer reaction and to the double layer charging processes. IEM includes the diffusion impedance Z_D in series with R_{ct} y C_{dl} in parallel.

2. THE MODEL

IEM is based on the model we previously published [14]–[15]. Now, it has incorporated the diffusion process of electroactive ions to the EEI. The model then, integrates in a same circuit, the electrochemical and the geometrical aspects of the electrode.

2.1. The Diffusion Impedance

The semi infinite linear diffusion of the ions to the EEI is a process which can be physically observed as the movement of charged particles that represent a non symmetric spatial distribution of electrical charge. The movement of charged ions produced by a concentration gradient generates current and consequently an energy dissipation which can be modelled as an electrical resistance R_D.

On the other hand, the concentration gradient is originated because the ions react when they reach at EEI. As result, a time-evolution of the concentration profile for species occurs. This asymmetric charge distribution can be seen and modelled electrically as a pseudo capacitance or distributed capacitance C_D. Given that both processes, loss of energy and uneven charge distribution occur simultaneously at the same place, it is appropriate to connect both electrical components in parallel.

This diffusion impedance (R_D // C_D) is incorporated on each level of the fractal net as it is shown in Fig. 2, since the thickness of the diffusion layer is way lower than the roughness dimensions. Back in 1980 Bard [20] already found experimentally that the thickness of the diffuse layer varies between 0.3 nm y 0.03 um respectively for concentrations from 100 mM/l to 0.1 mM/l.

In order to obtain R_D y C_D it is necessary to know the explicit form of concentration of the electrically active species. The problem is exposed on the appendix and an analytical solution is mathematically deduced for the semi infinite linear diffusion when the system is excited with low amplitude AC overpotential. It is considered that an O species is reduced on the electrode surface to another R species, and that at the beginning; only the O species is present in the solution at a C_0^b concentration.

A second order differential equation in partial derivatives for the concentration $C_o(x,t)$ is obtained from Fick's laws. It was considered that the current density associated with the charge transference should coincide with the current density associated with the diffusion process on the electrode surface by using appropriate border conditions.

The equation above is solved by using the Laplace Transformed method and the diffusion current density is calculated as $J_{Diff} = -zFD\left(\frac{\partial C_o(x,t)}{\partial x}\right)$ where z = species valence O, F = Faraday Constant y D = Diffusion Coefficient of the electroactive species. The diffusion current density consists of two terms that are in-phase and quadrature respectively with the overpotential applied. The component in-phase is associated with the energy dissipation, and the component in quadrature is associated with the reactive part of the diffusion impedance.

2.2. IEM

The electrical circuit derived on the structure of a fractal network of an EEI is shown in Fig. 2.

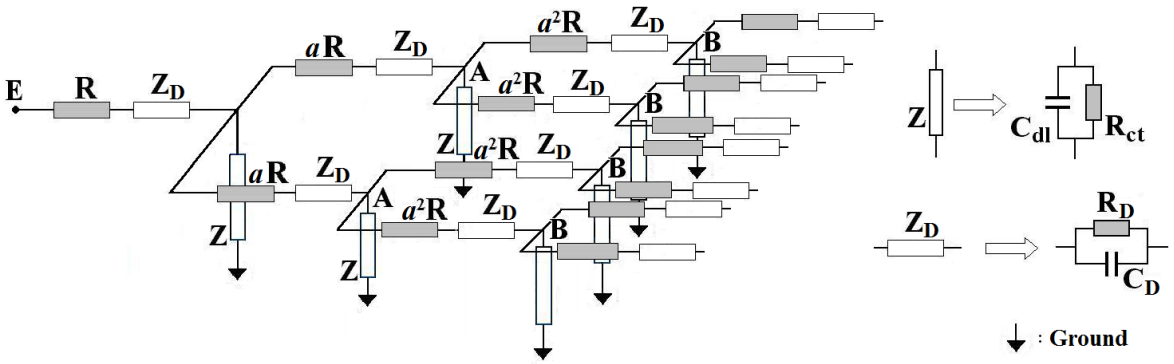

Figure 2. Tridimensional circuit model of an EEI fractal network. R_{ct} and C_{dl} idem to Fig.1. R: medium resistance of flat electrode (j=0; idem to Fig. 1), a: scale factor, R_D and C_D are diffusion resistance and capacitance respectively. A and B are equipotential points.

To develop the model they were not taken into account mass transfer processes by convection and migration, corrosion and surface adsorption. It was also considered a simple electron transfer reaction. Given that circuit components are the same in all branches, equipotential points at each fractal level can be assumed. E.g. A is the equipotential point for the first fractal level, B for the second and so on. From this equipotentiality, it is possible redraw the circuit as shown in Fig 3. In it, the following equations hold:

$$R_{Dj} = \frac{R_D}{2^j} \quad (1)$$

$$C_{Dj} = 2^j C_D \quad (2)$$

$$C_{dlj} = 2^j C_{dl} \quad (3)$$

$$R_{ctj}(\eta_j) = \left[2^j J_0 \frac{F}{RT}\left[(1-\beta_C)\exp\left(\frac{(1-\beta_C)F\eta_j}{RT}\right) + \beta_C \exp\left(\frac{-\beta_C F\eta_j}{RT}\right)\right]\right]^{-1} \quad (4)$$

Where R_D and C_D are given by equations (A29) y (A30) from the appendix, $\Re$= universal gas constant, J_0 = exchange current density, x = charge distribution thickness in the diffusion layer, β_c = cathodic transfer coefficient, T = absolute temperature and j = fractal level. If j=0 (fractal level 0) corresponds to a flat electrode. The R_{ctj} given by Eq. 4 was obtained by derivative of Butler–Volmer's Equation with respect to η_j (overpotential) and taking its inverse. The Butler–Volmer Equation is the fundamental relationship between current density and applied potential over an EEI.

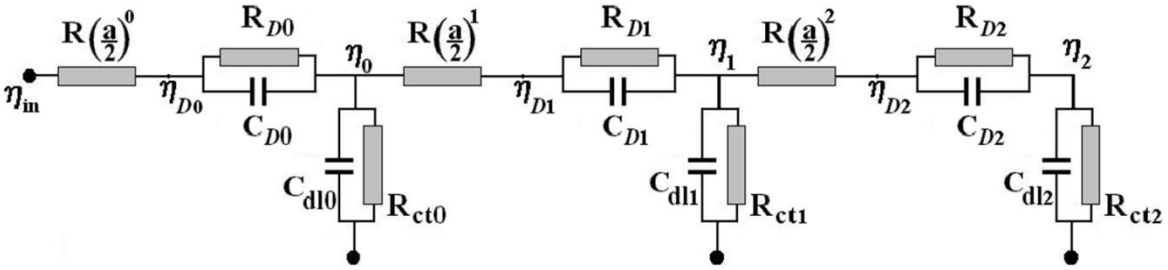

Figure 3. Redrawn fractal network showing its three first levels. η_j: overpotentials at different fractal levels.

2.3. Model's Series Equivalent Resistance and Reactance

The equivalent impedance of the model of Fig. 3 is shown in Eq. 5,

$$Z_{eq} = R + Z_{D0} + \frac{Z_0\left(\frac{aR}{2}+Z_{D1}+\frac{Z_1\left(\frac{a^2R}{4}+Z_{D2}+Z_2\right)}{Z_1+\frac{a^2R}{4}+Z_{D2}+Z_2}\right)}{Z_0+\frac{aR}{2}+Z_{D1}+\frac{Z_1\left(\frac{a^2R}{4}+Z_{D2}+Z_2\right)}{Z_1+\frac{a^2R}{4}+Z_{D2}+Z_2}} \quad (5)$$

Where Z_{Dj} and Z_j are the diffusion and EEI impedances respectively at the j-fractal level. The apparent area of the working electrode was considered as 1 cm^2. Then,

$$R_{eq} = Re(Z_{eq}) \quad (6)$$

$$X_{eq} = Im(Z_{eq}) \quad (7)$$

2.4. Req and Xeq Versus Time for an Alternating Overpotential

When an alternating overpotential η_{in} is applied on the EEI (Eq. 8), all overpotentials and R_{ctj}, will show periodic behaviours.

$$\eta_{in} = \eta_0 Sin(\omega t) \quad (8)$$

To obtain the time dependence of R_{eq} and X_{eq}, apply the second Kirchhoff's Law to the first node of the network (Fig. 3):

$$I_R = I_{R_{D0}} + I_{C_{D0}} \quad (9)$$

Given that,

$$I_{C_{D0}} = C_{D_0}\frac{d\left(\eta_{D_0}-\eta_0\right)}{dt} \quad (10)$$

It is obtained,

$$\frac{d\eta_{D_0}}{dt} = \frac{d\eta_0}{dt} + \frac{1}{C_{D_0}}\left(\frac{\eta_{in}-\eta_{D_0}}{R} - \frac{\eta_{D_0}-\eta_0}{R_{D0}}\right) \quad (11)$$

Analogously, repeating the above procedure on the next two nodes, it follows that:

$$\frac{d\eta_0}{dt} = \frac{1}{C_{dl0}}\left(\frac{\eta_{in}-\eta_{D_0}}{R} - \frac{\eta_0}{R_{ct0}} - \frac{2\left(\eta_0-\eta_{D_1}\right)}{aR}\right) \quad (12)$$

$$\frac{d\eta_{D_1}}{dt} = \frac{d\eta_1}{dt} + \frac{1}{C_{D_1}}\left(\frac{2\left(\eta_0-\eta_{D_1}\right)}{aR} - \frac{\eta_{D_1}-\eta_1}{R_{D1}}\right) \quad (13)$$

$$\frac{d\eta_1}{dt} = \frac{1}{C_{dl1}}\left(\frac{2\left(\eta_0-\eta_{D_1}\right)}{aR} - \frac{\eta_1}{R_{ct1}} - \frac{4\left(\eta_1-\eta_{D_2}\right)}{a^2R}\right) \quad (14)$$

$$\frac{d\eta_{D_2}}{dt} = \frac{d\eta_2}{dt} + \frac{1}{C_{D_2}}\left(\frac{4\left(\eta_1-\eta_{D_2}\right)}{a^2R} - \frac{\eta_{D_2}-\eta_2}{R_{D2}}\right) \quad (15)$$

$$\frac{d\eta_2}{dt} = \frac{1}{C_{dl2}}\left(\frac{4\left(\eta_1-\eta_{D_2}\right)}{a^2R} - \frac{\eta_2}{R_{ct2}}\right) \quad (16)$$

The set formed by Eqs. 11 to 16 constitute a differential equations system. Because this system cannot be solved analytically, it was used an algorithm similar to that employed in [14]–[15], but including some necessary changes to consider R_{Dj} and C_{Dj}.

3. RESULT

Typical values of the parameters were used for the simulation of IEM: β_C=0.5, T=298 ºK, f=1 10^{-4} Hz, f_{max}=10^4 Hz, η_{in}^0=5 mV, R=100 Ohms, x= 10^{-2}cm, D= 10^{-5} cm^2 s^{-1}, a=4, C_{dl}=1.10^{-5} F, J_0=7,3.10^{-6} A/cm^2, $\Re$=8.31 Joule mol^{-1} °K^{-1}.

3.1. Concentration of the electroactive species as a function of the time and distance to the electrode

Fig. 4 shows a 3D diagram which simulates the $C_O(x,t)$ evolution (Eq. A20), relative to the maximum concentration C_O^b, where x = distance to the electrode and t = time. It was considered that at first the solution only contains O species but not R ones. The diagram is an expansion of the profile concentration to which time has been added as a third axis. A low amplitude external alternating overpotential (5 mV) and low frequency (f = 0.01 Hz) is applied in t = 0.

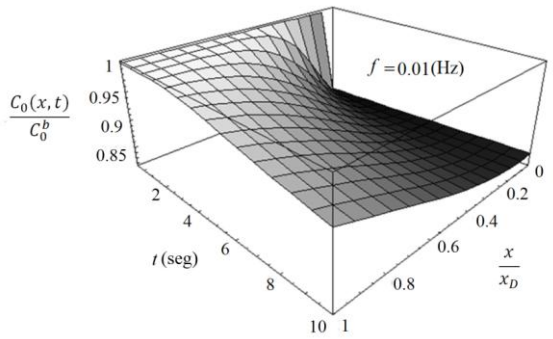

Figure 4. Species O concentration as function of x and t.

In a short time, O concentration shows a variation (from C_O^b initial value) for points close to the electrode, whereas for points at a distance in the order of the diffusion layer thickness, it differs a little from its value within the solution. As time passes on, the points far from the electrode show the disturbance effects and the concentration falls exponentially from C_O^b.

3.2. Dependence of Req and Xeq on the AC Overpotential Frequency

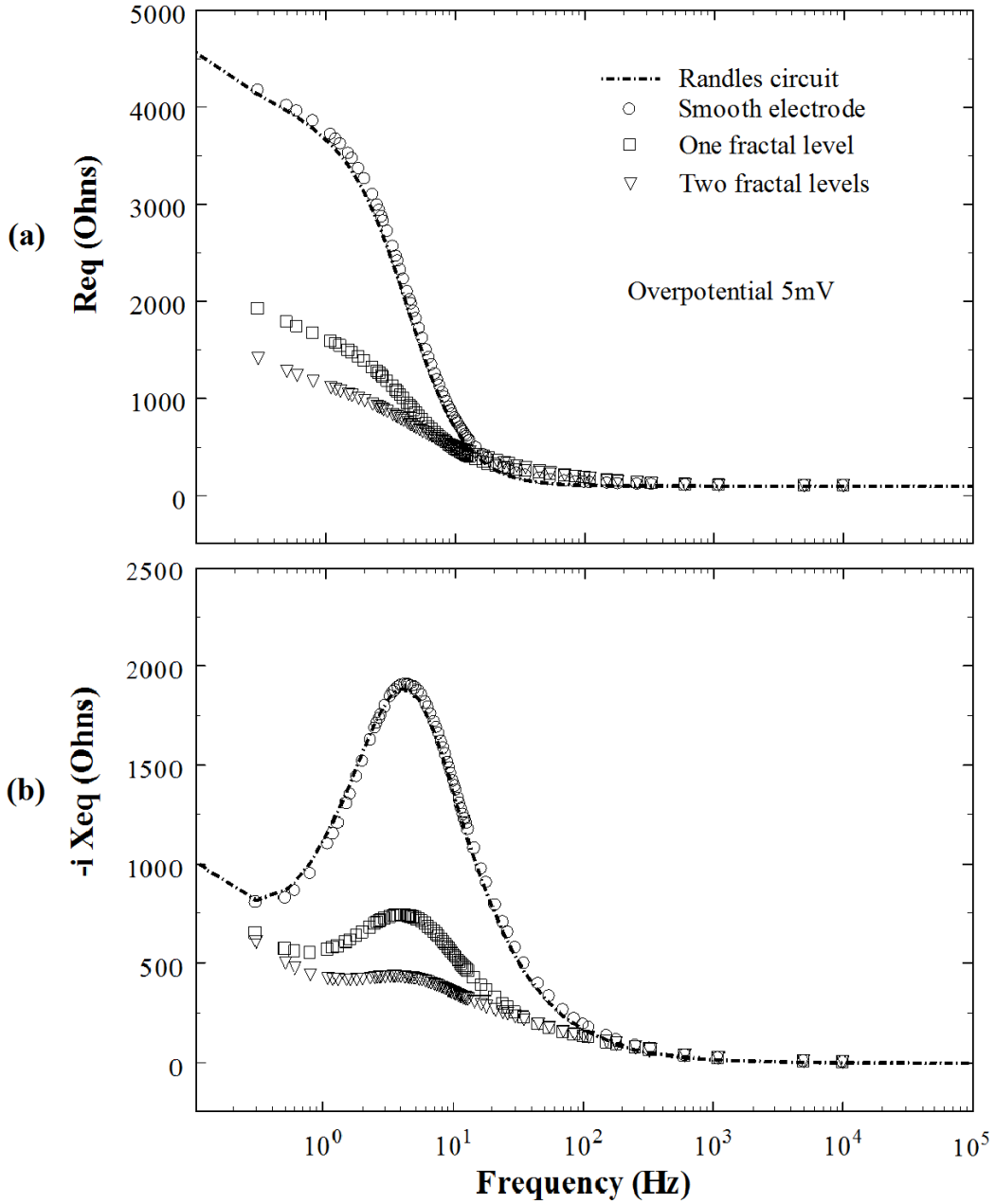

Figure 5. Dependence of R_{eq} (a) and X_{eq} (b) with frequency for Randles circuit and three nets: flat electrode and electrodes of one and two fractal levels. In all cases diffusion is included.

Fig. 5 shows the dependence of R_{eq} (a) and X_{eq} (b) average values on the applied overpotential frequency for Randles circuit and three networks (each corresponding to different fractal levels: j=0,1

y 2). In all cases diffusion is included. In the IEM case, this average values are computed as the null frequency component of the Fourier spectra of R_{eq} and X_{eq} temporal evolutions for each frequency. Typical parameters values were also used for the Randles circuit simulation: A_W=710 Ω $s^{-½}$, R=100 Ω, R_{ct}= 3615 Ω and C_{dl}=1.10-5 F. It is observed that for low frequencies, the R_{eq} and X_{eq} mean temporal values increase rapidly instead of approximating a constant and zero value respectively as it occurs when the diffusion is not present. It is observed within the central range and at high frequencies that the R_{eq} and X_{eq} mean temporal values show a similar behaviour to the one observed when diffusion was not considered.

3.3. Argand Diagram

The Argand diagram (Fig. 6) is also used to show the results presented in Fig. 5. In it the curves are frequency parametric. At frequencies lower than 0.1 Hz, the phase angle is 45º. At higher frequencies, the circular fitting of the rough electrode produces a depressed semicircular arch, which centre lies below the real axis. These fittings are not shown to clarify the figure. The Argand diagram of the flat electrode and the Randles's circuit don't show semicircles with sunken centre. This fact is well-marked in disperse systems' literature. [14]–[15]. To greater roughness of the electrode, the semicircles become smaller and distorted.

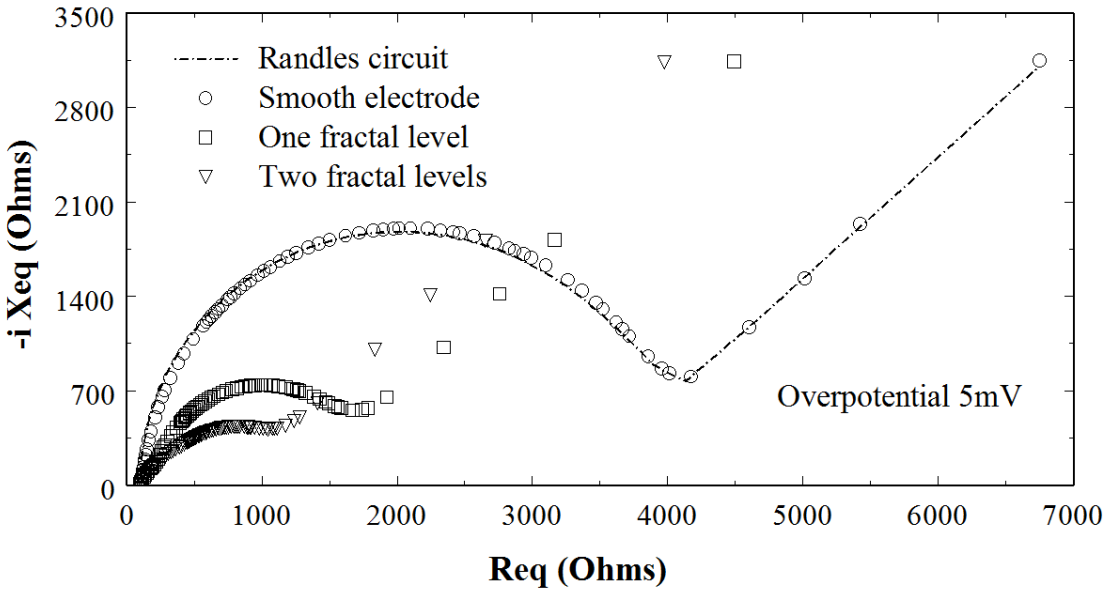

Figure 6. Argand Diagram for Randles circuit and three nets: flat electrode and electrodes of one and two fractal levels. In all cases diffusion is included.

It can observe that, within the frequency range where the diffusion is not significant (>0.1 Hz), R_{eq} and X_{eq} are decreased as roughness increases.

Whereas for frequencies, where there is a diffusion-controlled charge transfer (<0.1 Hz), the behaviour seems not to depend on the roughness and it gets closer to a 45° line on the graphic.

3.4. Discussion

The appendix shows in detail the deduction of the concentration $C_O(x,t)$ as a function of the distance to the electrode surface and time, for a semi infinite linear diffusion model. When the system is excited with low amplitude alternating overpotential, $C_O(x,t)$ is given by Eq. A20. It is a solution of a second order differential equation in partial derivative and it meets the imposed border conditions as it is shown in Fig. 4. Approximations to the concentration $C_O(x,t)$ [20]–[21] are presented in the literature. Particularly if $C_O(x,t)$ is evaluated in $x = 0$, the Eq. (17) is obtained.

$$C_O(0,t) = C_O^b + \frac{\sqrt{2} I_0 \eta_0}{\Re T \sqrt{D} \sqrt{\omega}} \left(\text{FresnelC}\left(\sqrt{\frac{2\omega t}{\pi}}\right) \text{Sin}(\omega t) - \text{FresnelS}\left(\sqrt{\frac{2\omega t}{\pi}}\right) \text{Cos}(\omega t) \right) \quad (17)$$

For a stationary state is reduced to:

$$C_O(x,t) = C_O^b + \frac{I_0 \eta_0}{\Re T \sqrt{D} \sqrt{2\omega}} \left(\text{Sin}(\omega t) - \text{Cos}(\omega t) \right) \quad (18)$$

This equation is the same expression presented in [21]. During the development, it has been found that the diffusion layer thickness x_d, by equation A24, depends on the inverse square root of the frequency. This would explain the higher the frequency, the lower the ion transit time to the electrode surface, and consequently, the lower longitude on the diffusion layer.

The function diffusion current density is obtained by derivation the concentration respect to the time, and particularized in $x = 0$ coincides with the current density of the charge transference process, thus, as expected, this event reflects Maxwell continuity equation.

The diffusion of electroactive species is not conceptually related to the charge transfer process, since these processes occur consecutively and in different places. Therefore, the electroactive species must necessarily diffuse previously to this interface so that these redox processes may occur in the interface. That is the reason why these processes have been modelled as series impedances.

De Levie [16] also showed the effect of roughness on electrodes in electrochemical measurement when it is considered the diffusion of the electroactive species to and from the electrode. Although the way the diffusion impedance is incorporated to the fractal net differs from our method, we have to remark that the results qualitatively coincide.

Kumar and Kant [22]–[23] reported the same dependence of the Warburg admittance with ω –when the charge transfer reaction is only governed by diffusion– as presented in this work.

Finally, when increasing the electrode roughness, the depressed centre semicircles decrease their size (Fig. 6). This is related to the corresponding decrease of equivalent charge transfer resistance.

3.5. Conclusions

The integral electrical model of an electrode-electrolyte interface here presented includes both geometrical and electrochemical aspects. The roughness degree of the electrode was modelled using a fractal structure. Two electrochemical aspects have been considered: The interface process and the diffusion process.

Analytical expressions for resistance (R_D) and diffusion reactance (X_D) have been formally deduced and included into IEM. These expressions represent the origin and nature of the diffusion process.

IEM proposes a more attractive interpretation of the physical processes; since it enables both a clearer differentiation between the ions movement into the EEI (charge transfer) and the ions movement into the diffusion layer, and a separately interpretation of the nature of these processes.

It must be highlighted that, while Randles circuit and the smooth electrode (j=0) have the same qualitative and quantitative behaviour; the underlying physical processes of each model are different.

Finally it is clear that, although both the Randles circuit and the IEM can qualitatively predict well the observed behaviour, they are still incomplete models. To solve this flaw, models of double layer voltage dependents, the surface adsorption process and the mass transport phenomena due to convection, must be incorporated.

APPENDIX

Impedance of a semi-infinite linear diffusion model:

A flat electrode is immersed in an electrolytic solution which only contains the electrochemically active species O, and its concentration is C_O^b. The R species is the reduced form of O on the electrode surface. The solution is supposed to be extended to the infinite. According to Fick's first law, the flux of substance O per unit area which diffuse through a parallel plane to the electrode at a distance x and in a perpendicular direction is directly proportional to the concentration gradient of substance O at that distance.

The proportionality factor D is the diffusion coefficient of the species O. If D is independent from both the concentration and x, Fick's second law can be expressed as shown in equation (A1):

$$\frac{\partial C_O}{\partial t} = D\frac{\partial^2 C_O}{\partial x^2} \qquad \text{(A1)}$$

In order to determine the function $C_O(x,t)$, we need to impose boundary conditions according to each situation.

In this paper the substance O distribution is regarded as uniform before the electrolysis, and its concentration is C_O^b (moles.cm^{-3}). We also consider that this concentration must reach this value when x tends to infinite. This condition can be expressed as follows:

$$C_O(x,0) = C_O^b \qquad \text{(A2)}$$

$$\lim_{x\to\infty} C_O(x,t) = C_O^b \qquad \text{(A3)}$$

The migration and convection processes are regarded as non-significant. When an alternating overpotential (η) with η_0 amplitude and f frequency is applied on the system (equation A4), the current density associated to the charge transference must coincide with the current density associated to the diffusion process on the surface of the electrode. This condition responds to current continuity.

$$\eta = \eta_0 \mathrm{Sin}(\omega t) \qquad \text{(A4)}$$

$$J_D = J_{ct} \qquad \text{(A5)}$$

J_{ct} is obtained from the Butler-Volmer equation, and considering that one electron is transferred in each electrochemical reaction:

$$J_{ct} = J_0\left[\left(1+\frac{(1-\beta_c)F\eta}{\Re T}\right)-\left(1-\frac{\beta_c F\eta}{\Re T}\right)\right] = J_0\frac{F\eta}{\Re T} \qquad \text{(A6)}$$

The diffusion current density is given by:

$$J_D = -FD\frac{\partial C_O}{\partial x} \qquad (A7)$$

Eq. (A8) is obtained by replacing Equations (A6) and (A7) in Eq. (A5)

$$-FD\frac{\partial C_O}{\partial x} = \frac{I_0 F}{RT}\eta_0 \mathrm{Sin}(\omega t) \qquad (A8)$$

The Laplace Transform of Equations (A1) and (A8) are respectively:

$$s\overline{C_O} - C_O^b = D\frac{\partial^2 \overline{C_O}}{\partial x^2} \qquad (A9)$$

$$-FD\frac{\partial \overline{C_O}}{\partial x}\Big|_{x=0} = \frac{I_0 F \eta_0}{RT}\frac{\omega}{s^2+\omega^2} \qquad (A10)$$

Eq. (A9) has the solution (complementary function + particular integral)

$$\overline{C_0}(x,s) = A\, e^{\sqrt{s/D}\,x} + B\, e^{-\sqrt{s/D}\,x} + \frac{C_O^b}{s} \qquad (A11)$$

A=0 when boundary conditions are accomplished and B is found by replacing Eq. (A11) in Eq. (A10). Therefore $\overline{C_0}(x,s)$ is:

$$\overline{C_0}(x,s) = \frac{I_0\eta_0}{RT\sqrt{D}}\frac{\omega\, e^{-\sqrt{s/D}\,x}}{(s^2+\omega^2)\sqrt{s}} + \frac{C_O^b}{s} \qquad (A12)$$

$C_0(x,s)$ is obtained by calculating the Inverse Laplace Transform from Eq. (A12). This Transform is obtained by applying Eq. (A13) twice.

$$\mathcal{L}^{-1}[f(s)\cdot g(s)] = \int_0^t F(u)\cdot G(t-u)\,du \qquad (A13)$$

Where $\mathcal{L}^{-1}$ symbolizes the inverse Laplace transform; *F* and *G* are the Laplace Transforms of *f* and *g*. Given that:

$$\mathcal{L}^{-1}\left[e^{-\sqrt{s/D}\,x}\right] = \frac{D\,x\,e^{-x^2/(4Dt)}}{2\sqrt{\pi}\sqrt{D^3t^3}} \qquad (A14)$$

$$\mathcal{L}^{-1}\left[\frac{I_0\eta_0}{RT\sqrt{D}\sqrt{s}}\right] = \frac{I_0\eta_0}{RT\sqrt{\pi D}\sqrt{t}} \qquad (A15)$$

It can be deduced that:

$$\mathcal{L}^{-1}\left[\frac{I_0\eta_0}{RT\sqrt{D}}\frac{e^{-\sqrt{s/D}\,x}}{\sqrt{s}}\right] = \frac{I_0\eta_0\, e^{-x^2/(4Dt)}}{RT\sqrt{\pi D}\sqrt{t}} \qquad (A16)$$

And because:

$$\mathcal{L}^{-1}\left[\frac{\omega}{s^2+\omega^2}\right] = \mathrm{Sin}(\omega t) \qquad (A17)$$

It follows that:

$$\mathcal{L}^{-1}\left[\frac{I_0\eta_0}{RT\sqrt{D}}\frac{e^{-\sqrt{s/D}\,x}}{\sqrt{s}}\frac{\omega}{s^2+\omega^2}\right] = \frac{I_0\eta_0}{RT\sqrt{\pi D}}\int_0^t \frac{e^{-x^2/(4Dt)}\mathrm{Sin}[\omega(t-u)]}{\sqrt{u}}du \qquad (A18)$$

Then the species O concentration at a distance *x* from the electrode and at an instant *t* is given by Eq. (A19).

$$C_0(x,t) = C_O^b + \frac{I_0\eta_0}{RT\sqrt{\pi D}}\int_0^t \frac{e^{-x^2/(4Dt)}\mathrm{Sin}[\omega(t-u)]}{\sqrt{u}}du \qquad (A19)$$

A solution for Eq. (A19) is:

$$C_0(x,t) = C_O^b - \frac{I_0\eta_0}{RT\sqrt{\pi D}}e^{-x^2/(4Dt)}\mathrm{Cos}(\omega t)\left[\frac{\sqrt{2\pi}x^2\sqrt{\omega}}{2D}\mathrm{FresnelC}\left(\sqrt{\frac{2\omega t}{\pi}}\right) + \sqrt{\frac{2\pi}{\omega}}\mathrm{FresnelS}\left(\sqrt{\frac{2\omega t}{\pi}}\right)\right] + \frac{I_0\eta_0}{RT\sqrt{\pi D}}e^{-x^2/(4Dt)}\mathrm{Sin}(\omega t)\left[\frac{\sqrt{2\pi}x^2\sqrt{\omega}}{2D}\mathrm{FresnelS}\left(\sqrt{\frac{2\omega t}{\pi}}\right) + \sqrt{\frac{2\pi}{\omega}}\mathrm{FresnelC}\left(\sqrt{\frac{2\omega t}{\pi}}\right) - \frac{x\sqrt{\pi}}{\sqrt{D}}\right] \qquad (A20)$$

Where:

$$\mathrm{FresnelC}(z) = \int_0^z \mathrm{Cos}\left(\frac{\pi}{2}t^2\right)dt \qquad (A21)$$

$$\mathrm{FresnelS}(z) = \int_0^z \mathrm{Sin}\left(\frac{\pi}{2}t^2\right) dt \qquad \text{(A22)}$$

The diffusion current density for a stationary state is obtained by replacing Eq. (A20) in Eq. (A7):

$$J_D = \frac{J_0 F \eta_0}{\Re T}\left[\frac{x\sqrt{2\omega}}{2\sqrt{D}}\mathrm{Cos}(\omega t) + \left(1 - \frac{x\sqrt{2\omega}}{2\sqrt{D}}\right)\mathrm{Sin}(\omega t)\right] \text{(A23)}$$

Both terms in Eq. (A23) must present the same frequency dependence so that the theoretical model may coincide with the experimental observation [1]. This condition is accomplished when x_D is:

$$x_D = \sqrt{D}/\sqrt{2\omega} \qquad \text{(A24)}$$

x_D could be interpreted as the charge distribution thickness in the diffusion layer. Eq. (A23) is written by replacing Eq. (A24) in Eq. (A23):

$$J_D = \frac{J_0 F \eta_0}{\Re T}\left[\frac{x\sqrt{2\omega}}{2\sqrt{D}}\mathrm{Cos}(\omega t) + \frac{\sqrt{2\omega}}{\sqrt{D}}\left(x_D - \frac{x}{2}\right)\mathrm{Sin}(\omega t)\right] \qquad \text{(A25)}$$

When $x \cong x_D$ equation (A25) is abridged to:

$$J_D = \frac{J_0 F \eta_0}{\Re T}\left[\frac{x_D\sqrt{2\omega}}{2\sqrt{D}}\mathrm{Cos}(\omega t) + \frac{x_D\sqrt{2\omega}}{2\sqrt{D}}\mathrm{Sin}(\omega t)\right] \text{(A26)}$$

Electrical model:

The diffusion occurs at the same place where two phenomena simultaneously take place. The first one is the space distribution of the species diffused. Since this species is electrically charged, it can be modelled as a pseudocapacitance or distributed capacitance. These charges generate energy dissipation as they move, and this energy can be associated to an electrical resistance. Since both phenomena occur at the same place simultaneously, they can be modelled as a circuit with capacitance and resistance connected in parallel. The circuit admittance is:

$$Y = \frac{1}{R_D} + i\omega C_D \qquad \text{(A27)}$$

Given that η is the applied overpotential

$$J_D = Y\eta \qquad \text{(A28)}$$

The electrical resistance R_D is associated with the current density in phase with the applied overpotential. Likewise, the capacitive reactance is associated with the current density in counterphase with the applied overpotential.

$$R_D = X_D = \frac{2\Re T\sqrt{D}}{F J_0 x}\frac{1}{\sqrt{2\omega}} \qquad \text{(A29)}$$

Then C_D is obtained using Eq. A27 as $(\omega X_D)^{-1}$:

$$C_D = \frac{F J_0 x\sqrt{2}}{2\Re T\sqrt{D}}\frac{1}{\sqrt{\omega}} \qquad \text{(A30)}$$

And the phase angle is $\phi = Tan^{-1}(R_D/X_D) = 45°$.

ACKNOWLEDGMENTS

This work was supported by grants from the Agencia Nacional de Promoción Científica y Tecnológica, the Consejo Nacional de Investigaciones Científicas y Técnicas (CONICET), the Consejo de Investigaciones de la Universidad Nacional de Tucumán (CIUNT), and by the Instituto Superior de Investigaciones Biológicas (INSIBIO). The authors would like to thank Professor Micaela García for her help in the language editing of this manuscript.

REFERENCES

1. E. Warburg, *Ann. Phys. Chim*., 67 **(**1899**)** 493-499.
2. J. Randles, *Disc. Faraday Soc*., 1 (1947) 11-19.
3. H. Fricke, *Phil. Mag*., 14 (1932) 310-318.
4. L. Geddes and L. Baker, L. E. in *Principles of Applied Biomedical Instrumentation*, **3**rd edition, edited by John Wiley, John Wiley, New York, 1989, Vol. 1, Chap. 13, p.853.
5. S. Taylor and E. Gileadi, *Corrosion, (NACE)*, 51 (1995) 664-671.
6. E. McAdams, J. Jossinet and A. Lackermeier, *Innov. Tech. Biol. Med*., 16, (1995) 662-670.
7. S. Liu, *Phys. Rev. Lett.*, 55 (1985) 529-532.
8. L. Nyikos and T. Pajkossy, *Electrochim. Acta*, 30 (1985) 1533-1540.
9. L. Nyikos and T. Pajkossy, *Electrochim. Acta*, 31 (1986) 1347-1350.
10. T. Pajkossy and L. Nyikos, *J. Electroanal. Chem.*, 332 (1992) 55-61.
11. T. Pajkossy and L. Nyikos, *New J. Chem.*, 14 (1990) 233-237.
12. T. Pajkossy, *J. Electroanal. Chem*., 300 (1991) 1-11.
13. T. Pajkossy, *Heterog. Chem. Rev.*, 2 (1995) 143-147.
14. G. Ruiz, C. Felice and M. Valentinuzzi, *Chaos Solitons &Fractals*, 25 (2005) 649-654.
15. G. Ruiz and C. Felice, *Chaos, Solitons & Fractals*, 31 (2007) 327-335.
16. R. De Levie, *J. Electroanal. Chem.*, 281 (1990) 1-21.
17. M. Finšgar, *Corrosion Science* 72 (2013) 82–89.
18. A. Ehsani, M. Mahjani, M. Bordbar and S. Adeli, *J. Electroanal. Chem.*, 710 (2013) 29-35.
19. M. Mahjani, A. Ehsani and M. Jafarian, *Synthetic Metals* 160 (2010) 1252–1258.
20. A. Bard and L. Faulkner, *Electrochemical methods*, New York, John Wiley & Sons, Inc., 1980.
21. Southampton Electrochemistry Group, in *Instrumental Methods in Electrochemistry*, edited by Ellis Horwood Limited, John Wiley and Sons, New York, 1985, Appendix, p.406.
22. R. Kumar and R. Kant, *J. Phys. Chem. C*, 113 (2009) 19558–19567.
23. R. Kumar and R. Kant, *J. Chem. Sci*., 121 (2009) 579–588.